

Living-Free-Radical Emulsion Photopolymerization of Methyl Methacrylate by a Surface Active Iniferter (Suriniferter)

Sang Eun Shim, Yoda Shin, Jong Won Jun, Kangseok Lee, Hyejun Jung, and Soonja Choe*

Department of Chemical Engineering, Inha University, 253 Yonghyundong, Namgu, Incheon, South Korea 402-751

Received March 17, 2003; Revised Manuscript Received August 11, 2003

ABSTRACT: A novel surface-active RAFT agent as a suriniferter, composed of the dithiobenzoyl main structure and a benzoic hydrophobic carboxylate hydrophilic moiety, was synthesized and applied to the living-radical emulsion polymerization of methyl methacrylate (MMA) initiated by UV irradiation in the absence of added surfactant and additional initiator at various temperatures. A stable spherical bead of PMMA was successfully obtained using the suriniferter, maintaining the living-radical polymerization characteristics. Monomer conversion, molecular weight evolution and distribution, and final particle sizes were characterized. The higher the iniferter concentration, the higher the conversion and the lower the molecular weight, final particle size, and molecular weight distribution (PDI) obtained. A linear increase in molecular weight with respect to conversion is observed, implying that this technique using the suriniferter follows living-radical polymerization. The PDI varies from 1.21 to 1.43, and the final particle sizes vary from 407 to 304 nm with an increase in the polymerization temperature from 60 to 80 °C. The ratios of the triad tacticity for syndiotactic, atactic, and isotactic configurations of the synthesized PMMA are 54.3, 38.6, and 7.1, respectively, and the glass-transition temperature (T_g) is 126.6 °C, which is much higher than that of commercial PMMA ($T_g = 105$ °C). Thus, it is believed that the suriniferter used in living-free-radical emulsion polymerization modifies the stereoregularity of the PMMA.

Introduction

With regard to the fast development of materials science, the use of polymeric materials has been extensive, and the design of proper polymeric materials at the molecular level has become very important. Owing to the advent of several revolutionized "living"-radical polymerization methods, synthesizing well-defined polymers/copolymers having a desired structure has come true in a convenient way; therefore, the subject of the molecular design of polymers by means of living-radical polymerization has been a rapidly growing research area. These methods mainly include nitroxide-mediated polymerization (NMP),^{1,2} atom-transfer radical polymerization (ATRP),^{3,4} and reversible addition-fragmentation chain-transfer polymerization (RAFT).^{5,6} Among them, the RAFT process has several advantages over NMP or ATRP. Unlike NMP or ATRP, RAFT can be easily applied to a variety of monomers at the same reaction temperature and with the same method as in conventional radical polymerization without the need for an additional catalyst-removal process.⁷ Therefore, the discovery of the RAFT process is a breakthrough in the field of living-radical polymerization.

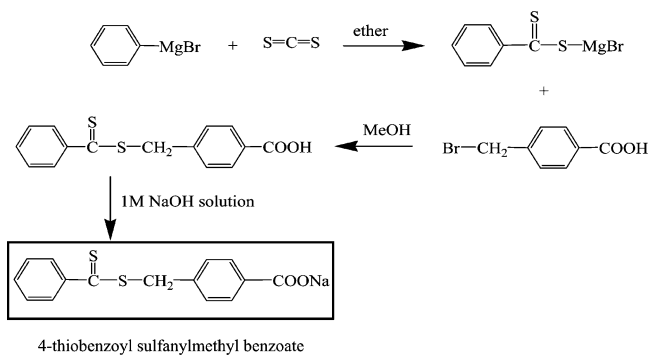
In general, the RAFT process uses various sulfide and disulfide *iniferters* (i.e., *initiator transfer-agent terminator*)⁸ in conjunction with conventional initiator to confer a living nature throughout the polymerization. Such iniferters are classified into photoiniferters bearing a dithiocarbamyl group^{9,10} and thermal iniferters carrying carbon-carbon^{11,12} or azo^{13,14} bonds according to the dissociation locus.

The initial interest in living-radical polymerization has been focused on the control of polymer molecular

architecture, and polymerization has been carried out in bulk or organic media. However, living-radical polymerizations carried out in aqueous media^{15,16} are of great importance in industrial application. Water as the reaction medium endows a number of advantages such as environmental-friendly processes, easy removal of reaction heat released during polymerization, and feasible handling of the final product because of its low viscosity.

Because RAFT can be readily applicable to emulsion or miniemulsion polymerization, intensive studies focused on conducting living-radical polymerization in a water medium have been carried out in this field.^{17–22} As with conventional emulsion polymerization process, typical ingredients for RAFT emulsion polymerization are water, water-insoluble monomers, water-soluble initiators, RAFT agents, and surfactants such as sodium dodecyl sulfate (SDS). The surfactant is responsible for the stability of the latex by preventing coagulation between particles. However, when SDS was used with RAFT agents in emulsion polymerization, it significantly retarded the polymerization rate and a deteriorated red layer of low-molecular-weight dormant species was observed at the beginning of polymerization, suggesting that SDS interacts with RAFT agents.²³ To overcome the problems induced by surfactant, addition-fragmentation reactive surfactant, so-called TRANSURF, has been designed; TRANSURF acts as both a chain-transfer agent and a surfactant in the RAFT emulsion polymerization of MMA.^{24,25} The basic structure of TRANSURF consists of three functional groups: methyl methacrylate dimer acting as a chain-transfer agent, a long aliphatic hydrocarbon chain responsible for the hydrophobic moiety, and a sulfate group attached to the hydrocarbon chain for hydrophilicity.

* Corresponding author. E-mail: schoe@inha.ac.kr. Tel: +82-32-860-7467. Fax: +82-32-876-7467.

Scheme 1. Synthesis of 4-Thiobenzoyl Sulfanylmethyl Benzoate

In this study, a novel surface-active RAFT agent, so-called suriniferter, composed of the dithiobenzoyl main structure, a benzoic hydrophobic moiety, and a carboxylate hydrophilic moiety was synthesized and applied to the RAFT emulsion polymerization of MMA initiated by UV irradiation in the absence of added surfactant and without additional initiator. Then, the suriniferter concentration and temperature-dependent polymerization characteristics such as the conversion, molecular weight and distribution, final particle size, and structural regularity of PMMA latex were studied.

Experimental Section

Materials. Reagent-grade phenylmagnesium bromide, α -bromo-*p*-toluic acid, and carbon disulfide used in the preparation of suriniferter were purchased from Aldrich (Milwaukee, WI). Anhydrous diethyl ether and methanol were purchased from J. T. Baker Co. (Phillipsburg, NJ). Carbon disulfide and diethyl ether were distilled to remove existing impurities and water. MMA (Junsei Chemicals, Japan) was distilled under reduced pressure to remove inhibitors and was stored in a refrigerator prior to use. Double-distilled deionized (DDI) water was used as a reaction medium.

Synthesis of Suriniferter. 4-Thiobenzoyl sulfanylmethylsodium benzoate suriniferter was synthesized in three steps. First, 0.03 M phenylmagnesium bromide and 0.045 M carbon disulfide reacted in dry diethyl ether at 10 °C for 6 h. After removing unreacted reagents by distillation, a 1.7:1 molar ratio of (thiobenzoyl)sulfanylmagnesium bromide to α -bromo-*p*-toluic acid was added to methanol. The second step in the reaction was carried out at 60 °C for 24 h. Again, unreacted reagent and methanol were removed by distillation. The $-\text{COOH}$ end group of the product obtained from the second step was replaced by $-\text{COONa}$ via a 1 M NaOH solution that was used to introduce water solubility into the product so that it could be used in emulsion polymerization. Details of the synthesis procedure of the suriniferter are shown in Scheme 1.

Polymerization of MMA. Polymerization was carried out in a 500-mL three-necked reaction vessel equipped with a mechanical stirrer. The agitation speed was kept at 150 rpm. Polymerization temperatures were 60, 70, and 80 °C and were controlled by a water-bath circulator; a nitrogen atmosphere was maintained throughout the polymerization. A 1-kW UV lamp having a 365-nm wavelength was employed to initiate the polymerization. The methyl methacrylate (MMA) concentration was 10 wt % based on the reaction medium, and the initiator concentration was varied from 0.1×10^{-3} to 1.0×10^{-3} M. The general procedure was as follows: DDI water and MMA were combined in a reaction vessel and purged with nitrogen for 30 min. When the temperature inside the reaction vessel reached the desired level, the vessel was charged with suriniferter dissolved in a small amount of water, and the reaction was initiated by turning on the UV lamp. During the 6-h polymerization, 5 mL of the sample was periodically taken from the reaction vessel in order to characterize the polym-

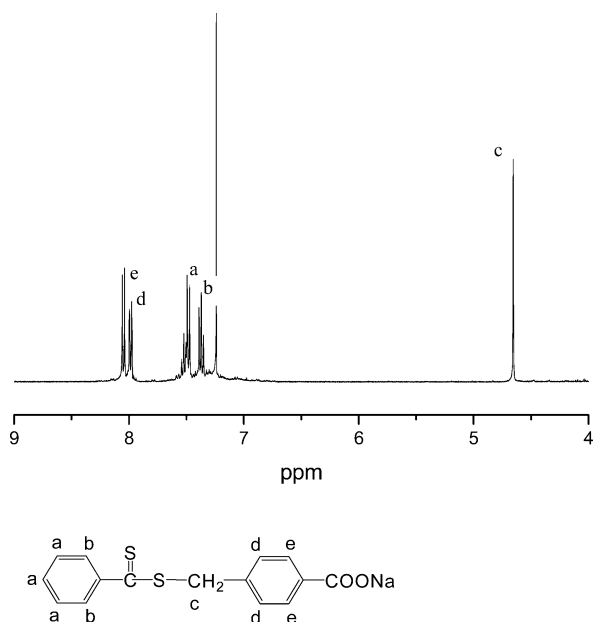


Figure 1. ^1H NMR spectrum of the synthesized suriniferter.

erization products, including conversion, molecular weight and distribution, and intermediate particle morphology. After the completion of polymerization, the resultant latex was frozen in a refrigerator and became molten at room temperature. The precipitated phase was collected and dried in vacuo for 24 h. As a consequence, white PMMA beads were obtained.

Characterizations. The chemical structures of the synthesized suriniferter and the obtained PMMA were confirmed with a Varian 400-MHz ^1H NMR using CDCl_3 as the solvent. The molecular weight and polydispersity index (PDI) were characterized using Waters GPC (gel permeation chromatography) equipped with a 510 differential refractometer and a Viscotek T50 differential viscometer. High-resolution 10^5 , 10^3 , and 10^2 Å μ -styragel packed columns were employed. A universal calibration curve was obtained on the basis of 10 polystyrene standard samples (Polymer Laboratories, U.K.) with molecular weights ranging from 7 500 000 to 580 g/mole. PMMA powder dissolved in THF was injected at a flow rate of 1.0 mL/min. Scanning electron microscopy (SEM, Hitachi S-4300) was used to study the morphology of the synthesized PMMA particles. Differential scanning calorimetry (DSC, Perkin-Elmer DSC-7) was used to investigate the glass-transition temperature of PMMA. The monomer conversion to polymer was determined gravimetrically. The number-average particle diameter, D_n was obtained using Scion Image Analyzer Software by counting 100 individual particles from SEM microphotographs.

Results and Discussion

Scheme 1 shows the synthesis of 4-thiobenzoyl sulfanylmethylsodium benzoate for the RAFT agent as a suriniferter. The color of the reaction solution turned orange after the completion of the first step of the reaction, and the final pink powder was obtained after purification by distillation. The chemical structure of 4-thiobenzoyl sulfanylmethylsodium benzoate was confirmed from the proton NMR spectrum as shown in Figure 1. Scheme 2 represents the polymerization mechanism of this type of suriniferter in which the methyl benzoate group acts as an active growing species. In the absence of a conventional initiator such as potassium persulfate or ammonium persulfate, the generation of free radicals is ascribed to the suriniferter because it plays the role of initiator. Therefore, the term "iniferter" proposed by Otsu⁸ would be appropriate in the absence of a conventional initiator. In this case, a

Scheme 2. RAFT Mechanism of MMA (M) in the Presence of Suriniferter

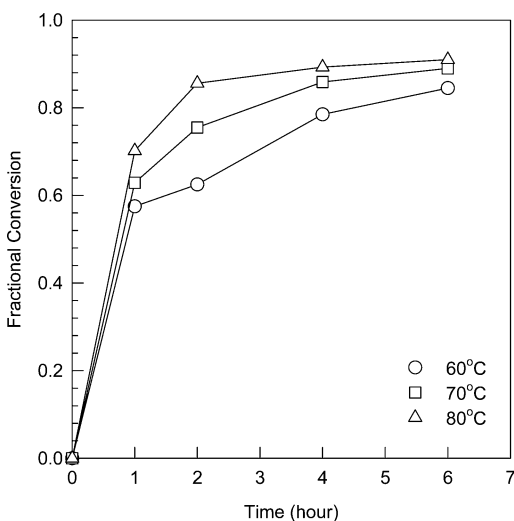
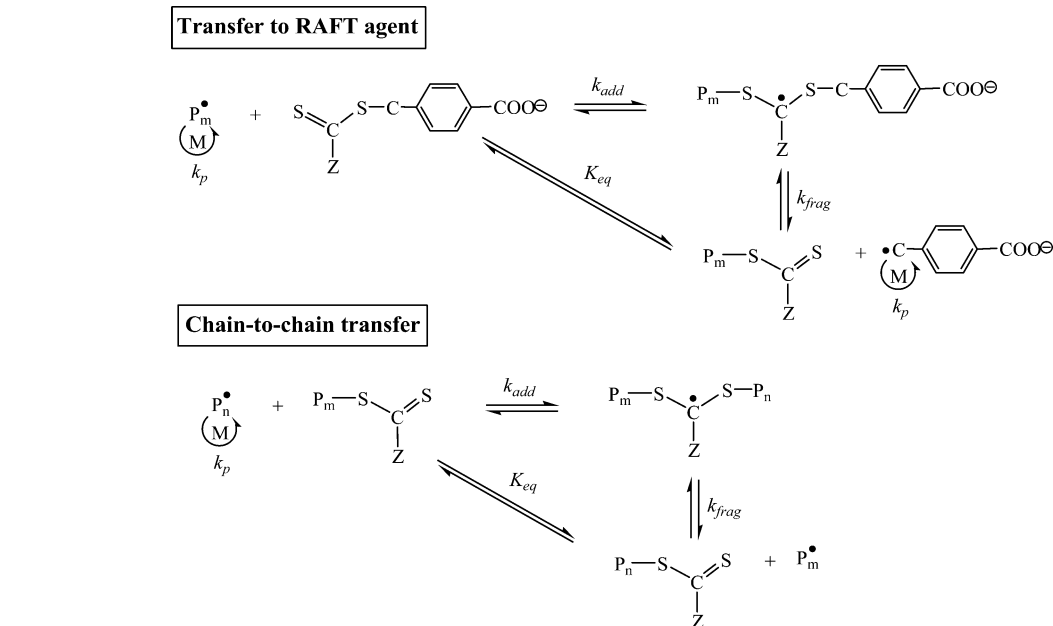


Figure 2. Fractional conversion vs reaction time with a suriniferter concentration of 0.5×10^{-3} M at various temperatures.

radical is produced from the iniferter, and the active radical is transferred to the iniferter itself; then a growing species is generated by a reversible addition-fragmentation mechanism. The active growing moiety further reacts with monomer, and the radical is transferred to the dormant chain with the dissociation of another radical that induces termination. However, in the presence of initiator, the iniferter would rather act as a chain-transfer agent, so the "RAFT agent" would be appropriate. Under UV irradiation of dithioester compounds, Hong et al.²⁶ suggested a reversible termination mechanism as an explanation of living behavior. However, Quinne et al.²⁷ claimed that the reversible termination mechanism was not adequate compared to the RAFT mechanism because it was not enough to differentiate between the two mechanisms regarding the structure of the polymer obtained and account for the fate of radicals generated in the monomer.

Polymerization Characteristics and Formation of a Stable PMMA Colloid. Figure 2 shows the effect of polymerization temperature on the fractional conver-

sion of MMA with respect to polymerization time with 0.5×10^{-3} M suriniferter where initiation was introduced by UV irradiation. Because the suriniferter acts as an initiator, chain-transfer agent, terminator, and surfactant, the polymerization recipe simply consists of water, monomer, and the suriniferter. The plot of conversion versus polymerization time is similar to those in conventional emulsion polymerization. Conversions of 0.85, 0.89, and 0.91 for 6 h were obtained at 60, 70, and 80 °C, respectively. The higher the temperature, the higher the conversion obtained due to the fast propagation of the free radicals and possibly due to the fast decomposition of suriniferter at elevated temperature. In conventional radical polymerization, it is known that the activation energy for radical propagation is appreciably higher than that of termination at higher temperature.²⁸ Thus, the increase in k_p/k_t (k_p and k_t represent the rate constants at propagation and termination, respectively) with temperature results in a fast polymerization rate.

In Figure 3a, the number-average molecular weights of PMMA in the course of polymerization prepared by a constant 0.5×10^{-3} M suriniferter are shown as a function of conversion. It is noted that approximate 60% conversion was obtained at a very early stage (within 1 h) in the polymerization. Because the polymerization was so rapid in the beginning stage of the reaction, samples were taken after 1 h to avoid the artificial retardation of the polymerization by turning off the UV lamp. However, it is believed that the living nature is valid for the beginning stage of the polymerization because the extrapolated lines of the experimental data points pass through the origin for all systems.

The higher the polymerization temperature, the higher the achieved molecular weight, which is opposite to macroemulsion polymerization using thermal initiators.²⁹ In emulsion polymerization using conventional thermal initiators, the molecular weight tends to decrease with initiator concentration because high temperature induces a high concentration of free radicals introduced by the decomposition of the thermal initiator, which facilitates bimolecular termination. The same trend was reported for the living-free-radical polymer-

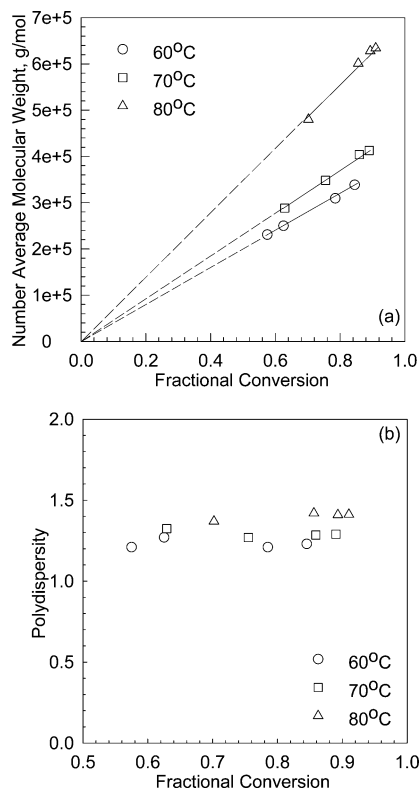


Figure 3. (a) Number-average molecular weight and (b) polydispersity vs conversion of PMMA prepared with 0.5×10^{-3} M suriniferter.

ization of polystyrene using a RAFT agent by thermal initiation at a series of temperatures: the number-average molecular weight decreases with temperature³⁰ for this reason. For the controlled radical polymerization of styrene and acrylate by an alkyl iodide degenerative transfer agent in the presence of AIBN, the dependence of molecular weight on polymerization temperature ranging from 50 to 90 °C was found to be weak.³¹

In general radical polymerization, the dependence of the rate of polymerization (R_p) and number-average degree of polymerization (\bar{x}_n) on temperature is expressed as follows:

$$\frac{d \ln(R_p)}{dT} = \frac{(2E_p + E_d) - E_t}{2RT^2} \quad (1)$$

$$\frac{d \ln(\bar{x}_n)}{dT} = \frac{2E_p - (E_d + E_t)}{2RT^2} \quad (2)$$

where, E_p , E_d , and E_t indicate the activation energy of propagation, initiator dissociation, and termination, respectively. R and T denote the gas constant and the temperature. Because the general order of magnitude of the activation energy is $E_d \gg E_p > E_t$, $(d \ln(R_p)/dT)$ and $(d \ln(\bar{x}_n)/dT)$ become positive and negative, respectively, when thermally decomposable initiator is involved, whereas they become both positive in the absence of thermal initiator (i.e., $E_d \approx 0$). In addition, photopolymerization follows the latter case³² where elevated temperature yields a high rate of polymerization and a high number-average degree of polymerization, which is directly related to the number-average molecular weight.

The polydispersity of PMMA during polymerization with respect to polymerization temperature at a fixed

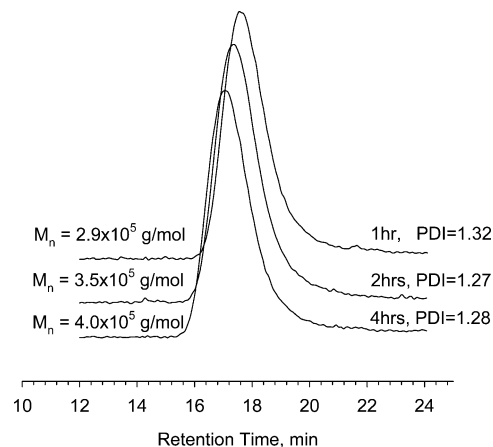


Figure 4. GPC traces for PMMA prepared by UV initiation with 0.5×10^{-3} M suriniferter at 70 °C.

suriniferter concentration of 0.5×10^{-3} M is depicted in Figure 3b. The final polydispersity index values are 1.23 (0.845 conversion), 1.29 (0.89 conversion), and 1.41 (0.91 conversion) at 60, 70, and 80 °C, respectively. The polydispersity tends to increase slightly with conversion and decrease with decreasing polymerization temperature. Ray et al. reported the decrease in PDI with respect to conversion both from experiment and simulation.³³ However, Quinn et al. found that the polydispersity index in RAFT polymerization initiated with UV radiation increased because of the degradation of the RAFT agent by UV at prolonged polymerization time.²⁷ In this study, the initiation was also achieved by UV radiation; therefore, an increase in PDI with conversion is expected because of the possible degradation of the RAFT agent.

The evolution of the molecular weight and polydispersity of PMMA prepared with 0.5×10^{-3} M suriniferter at 70 °C as a function of polymerization time is shown in Figure 4. It is clearly seen that the GPC chromatogram shifts to slightly low retention time owing to increasing number-average molecular weight but that the polydispersity is not influenced very much upon polymerization.

Figure 5 displays the SEM microphotographs of the PMMA beads prepared by living-radical emulsion polymerization at 0.5×10^{-3} M suriniferter at 60, 70, and 80 °C. Again, it should be noted that additional surfactant or initiator such as potassium persulfate (KPS) was not involved. In the presence of surfactant, polymer particles are formed in spherical micelles and continuously grow in size by monomer transport from droplets that acts as a monomer reservoir. In surfactant-free emulsion polymerization, hydrophilic sulfate free radicals generated by the decomposition of persulfate react with hydrophobic monomer dissolved in the aqueous phase to form oligomeric free radicals, which can play a role in micelle formation.³⁴ The mechanism for the subsequent particle growth is the same as that in the case where a surfactant is employed. Surfactants are composed of hydrophobic and hydrophilic parts. Examples of the hydrophobic moiety are long straight or branched alkyl groups, alkylbenzenes, and alkylnaphthalenes. Examples of the hydrophilic moiety include carboxyl ($\text{RCOO}^- \text{M}^+$), sulfonate ($\text{RSO}_3^- \text{M}^+$), or sulfate ($\text{ROSO}_3^- \text{M}^+$) for anionic surfactants and quaternary ammonium halides ($\text{R}_4\text{N}^+ \text{Cl}^-$) for cationic surfactants.³⁵ For 4-thiobenzoyl sulfanylmethylsodium benzoate used in this study, the surface-active group consists of

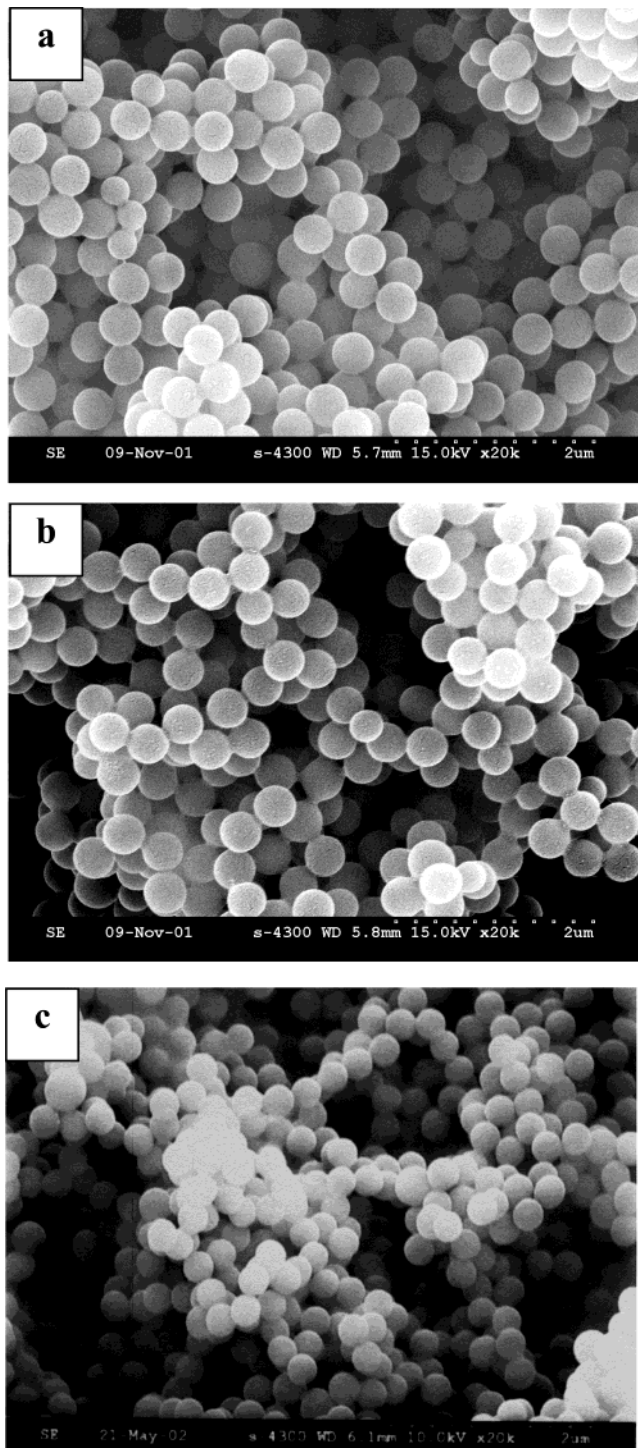


Figure 5. SEM micrographs of PMMA beads prepared with 0.5×10^{-3} M suriniferter at (a) 60, (b) 70, and (c) 80 °C.

hydrophobic benzyl and hydrophilic carboxyl moieties. By the homolytic cleavage of the carbon–sulfur bond in the suriniferter by UV irradiation, the methyl benzoate radical as an active growing species initiates polymerization. The benzyl group in the surfactant moiety in the suriniferter seems to be too short to play the role of surfactant in emulsion polymerization. However, as the length of the oligomeric radical bearing the carboxyl end group becomes longer by the further reaction of MMA, the degree of hydrophobicity tends to increase because the carbon–carbon bond in the oligomeric main chain is hydrophobic. This mechanism is similar to surfactant-free emulsion polymerization, as

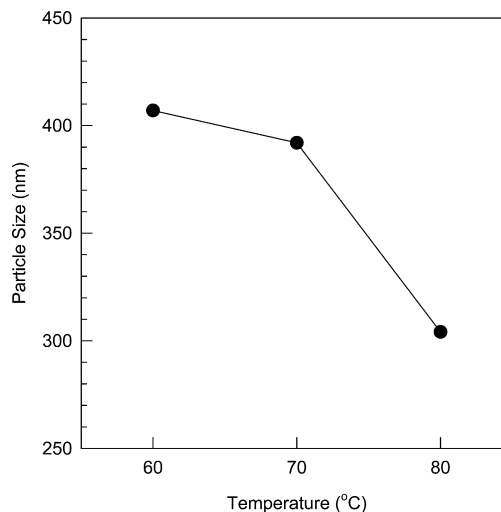


Figure 6. Effect of temperature on the final particle size of PMMA prepared with 0.5×10^{-3} M suriniferter.

Table 1. Influence of Suriniferter Concentration on Polymerization Characteristics and Particle Size for Preparation at 70 °C for 4 Hours

suriniferter conc (M)	M_n (g/mol)	PDI	conversion	particle size (nm)
0.1×10^{-3}	413 000	1.394	0.82	412
0.5×10^{-3}	404 000	1.321	0.89	392
1.0×10^{-3}	365 000	1.293	0.92	383

explained earlier. The production of stable spherical PMMA beads prepared in this study is thus attributed to the suriniferter carrying the carboxyl group.

Figure 6 represents the change in diameter of PMMA beads shown in Figure 5. In accordance with the temperature increase from 60 to 80 °C, the particle size decreases from 407 to 304 nm, which results in a common observation in emulsion polymerization.

The influence of the suriniferter concentration and the resultant particle diameter are tabulated in Table 1. As the suriniferter concentration increases from 0.1×10^{-3} to 1.0×10^{-3} M, the number-average molecular weight, the polydispersity, and the average particle size decrease, whereas the conversion increases, exhibiting the same behavior as observed when thermal initiator is used in conventional or RAFT emulsion polymerization. Regarding the reduced particle size, the concentration of suriniferter and RAFT radical transport should be considered. The increased amount of initiator (suriniferter in this work) induces a large number of polymeric particles, which leads to small individual particle sizes. Besides this effect, in the RAFT living-radical emulsion polymerization of styrene¹⁹ and butyl acrylate,³⁶ the number-average diameter was reported to decrease and the size distribution became narrower as the concentration of RAFT agent increased. This result was postulated by the fact that the active growing radicals produced from the fragmentation of the RAFT agent (or iniferter) exit the particles and reenter micelles to create new particles during the nucleation period in interval I of the emulsion polymerization mechanism. Gilbert et al. reported that the radical exit rate coefficient truly increased with increasing amounts of RAFT agent, resulting in a retardation of polymerization because of the transport of RAFT-agent radicals to the particles where polymerization is taking place.¹⁸

Figure 7 displays SEM microphotographs of PMMA beads prepared by 0.1×10^{-3} , 0.5×10^{-3} , and $1.0 \times$

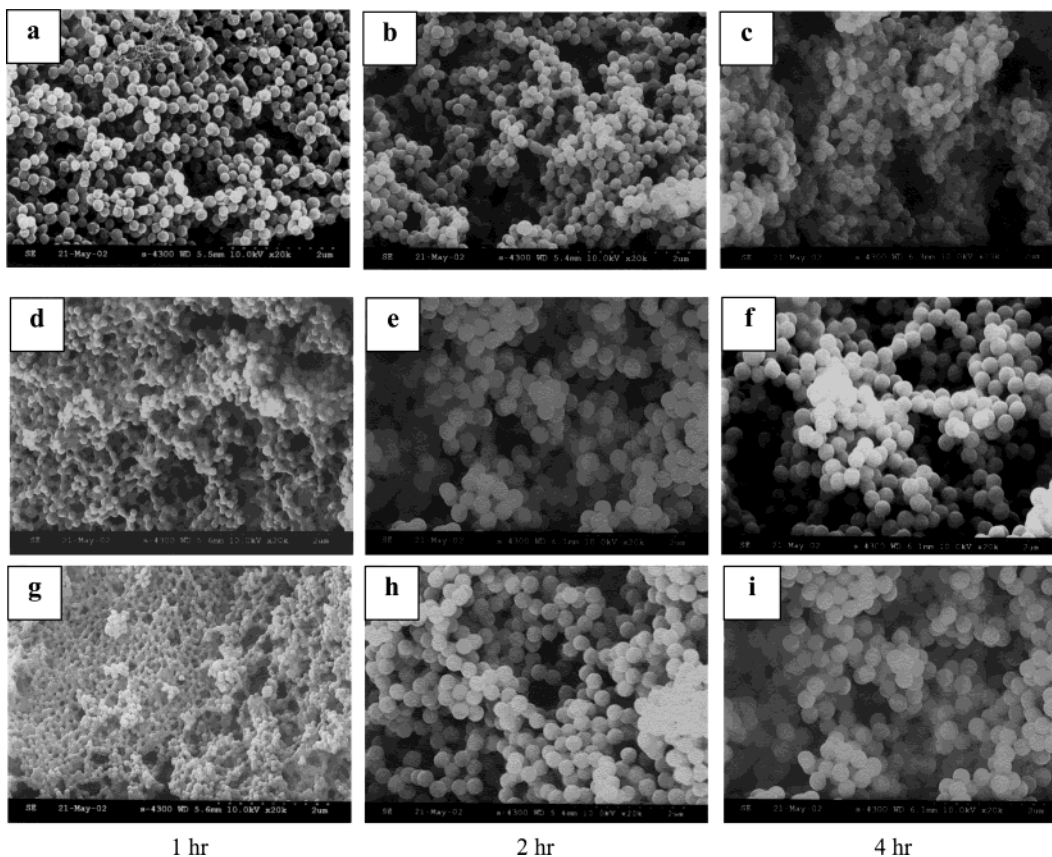


Figure 7. SEM micrographs of PMMA beads prepared with various amounts of suriniferter at 1, 2, and 4 h at 80 °C. (a) 0.1×10^{-3} M, 1 h; (b) 0.1×10^{-3} M, 2 h; (c) 0.1×10^{-3} M, 4 h; (d) 0.5×10^{-3} M, 1 h; (e) 0.5×10^{-3} M, 2 h; (f) 0.5×10^{-3} M, 4 h; (g) 1.0×10^{-3} M, 1 h; (h) 1.0×10^{-3} M, 2 h; and (i) 1.0×10^{-3} M, 4 h.

10^{-3} M suriniferter concentrations at 1, 2, and 4 h at 80 °C. In all cases, stable spherical PMMA beads are successfully produced. These particles are formed in an early stage of polymerization and subsequently grow. Because the conversions are different with respect to suriniferter concentration (i.e., a lower concentration of suriniferter yields a low conversion), it is not reasonable to compare the particle sizes depending on the polymerization duration. On the basis of Figure 7, it is seen that the suriniferter used in this study produces stable PMMA colloids without any additional surfactant or initiator.

Properties of PMMA Latex. The ^1H NMR spectrum of PMMA prepared with 1.0×10^{-3} M of suriniferter at 80 °C is seen in Figure 8; it shows three distinct peaks appearing at the highest field, which represent methacrylate methyl groups of different tacticity.³⁷ The bands at about 0.82, 1.02, and 1.18 ppm arise from syndiotactic (rr), atactic (mr), and isotactic (mm) methyl groups, respectively.³⁷ From Figure 8, the tacticity of the PMMA was calculated from the integrated ratios of rr, mr, and mm. The ratios of the triad tacticity for syndiotactic, atactic, and isotactic are 54.3, 38.6, and 7.1, respectively. The relatively regular molecular structure of the PMMA particles was expected to affect the thermal properties or characteristics. From Figure 9, we have observed that the glass-transition temperature (T_g) of the obtained PMMA is about 126.6 °C, which is much higher than that of commercial PMMA ($T_g = 105$ °C).³⁸ The syndiotacticity of the PMMA sample prepared in this study is 54.3%, which is higher than that of commercial PMMA bearing 43%.³⁸ The higher ratio of syndiotacticity results in a relatively regular structure and leads to an increase

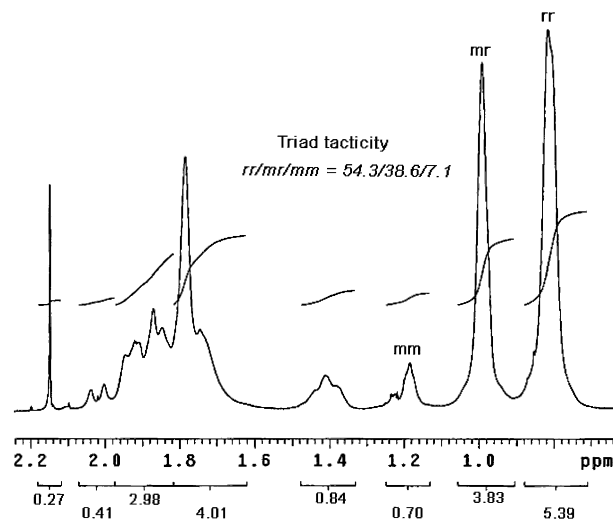


Figure 8. ^1H NMR spectrum of the obtained PMMA.

in the glass-transition temperature. It has been known that the glass-transition temperature of PMMA greatly depends on the tacticity of the polymer. In general, the glass-transition temperature of PMMA is proportional to the degree of syndiotacticity and inversely proportional to the degree of isotacticity. The glass-transition temperature of PMMA was reported to increase from 41.5 to 125.6 °C for syndiotacticity/atacticity/isotacticity triads of 0/5/95 and 64/36/9.³⁹

Thus, we believe that the use of suriniferter with living-free-radical emulsion photopolymerization can induce different tacticity in PMMA. This is the first observation in the present study. However, the exact

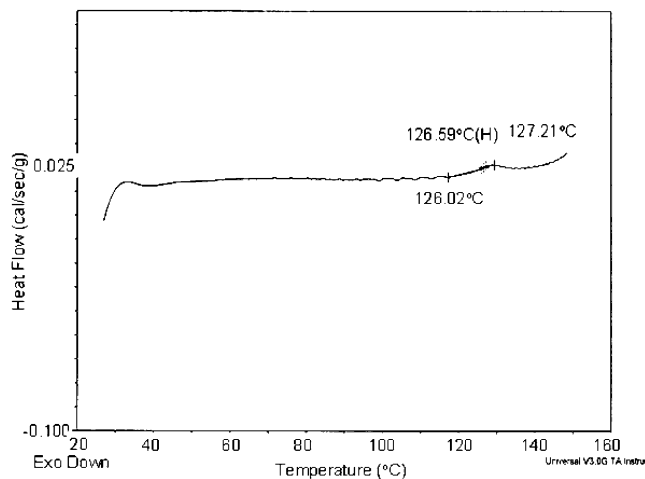


Figure 9. DSC thermogram of the prepared PMMA beads.

mechanism for the variance in the tacticity is not yet clarified; therefore, it is under investigation.

Conclusions

A novel surface-active RAFT agent as a suriniferter, composed of 4-thiobenzoyl sulfanylmethylsodium benzoate, was successfully synthesized and applied to the RAFT emulsion polymerization of methyl methacrylate initiated by UV irradiation in the absence of added surfactant or additional initiator. The suriniferter concentration and temperature-dependent polymerization characteristics such as the conversion, molecular weight and distribution, final particle size and distribution, and molecular regularity were studied. The higher the iniferter concentration, the higher the conversion and the lower the molecular weight and molecular weight distribution (PDI) and final particle size obtained. A linear increase in molecular weight with respect to conversion is observed, implying that this technique using suriniferter follows living-radical polymerization. The PDI varies from 1.21 to 1.43, and the final particle sizes vary from 407 to 304 nm with an increase in polymerization temperature from 60 to 80 °C. The ratios of the triad tacticity for the syndiotactic, atactic, and isotactic synthesized PMMA are 54.3, 38.6, and 7.1, respectively, and the glass-transition temperature (T_g) is 126.6 °C, which is much higher than that of the commercial PMMA ($T_g = 105$ °C) having 44% syndiotacticity. Higher ratios of syndiotacticity result in relatively regular structure, hence leading to an increase in the glass-transition temperature. Thus, it is believed that the suriniferter used in living-free-radical emulsion polymerization modifies the tacticity of PMMA.

Acknowledgment. This work was supported by an NRL (National Research Laboratory of the Ministry of Science and Technology in Korea) project (grant no. M10203000026-02J0000-01410, 2002–2007) and was partially supported by the Korea Research Foundation (grant no. KRF-2001-041-E00500).

References and Notes

- (1) Solomon, D. H.; Rizzardo, E.; Cacioli, P. U.S. Patent 4,581,429, 1986.
- (2) Georges, M. K.; Veregin, R. P. N.; Kazmaier, P. M.; Hamer, G. K. *Macromolecules* **1993**, *26*, 2987.

- (3) Kato, M.; Kamingaito, M.; Sawamoto, M.; Higashimura, T. *Macromolecules* **1995**, *28*, 1721.
- (4) Wang, J. S.; Matyjaszewski, K. *Macromolecules* **1995**, *28*, 7901.
- (5) Moad, G.; Chiefari, J.; Chong, Y. K.; Krstina, J.; Mayadunne, R. T. A.; Postma, A.; Rizzardo, E.; Thang, S. H. *Polym. Int.* **2000**, *49*, 993.
- (6) de Brouwer, H.; Monteiro, M. J.; Tsavalas, J. G.; Schork, F. J. *Macromolecules* **2000**, *33*, 9239.
- (7) *Controlled/Living Radical Polymerization, Progress in ATRP, NMP, and RAFT*; Matyjaszewski, K., Ed.; ACS Symposium Series 768; American Chemical Society: Washington, DC, 2000; p 23.
- (8) Otsu, T.; Yoshida, M. *Makromol. Chem. Rapid Commun.* **1982**, *3*, 127.
- (9) Otsu, T.; Matsunaga, T.; Doi, T.; Matsumoto, A. *Eur. Polym. J.* **1995**, *31*, 67.
- (10) Otsu, T.; Nayatani, K. *Makromol. Chem.* **1958**, *27*, 149.
- (11) Bledzki, T.; Brawn, D.; Titzschkau, K. *Makromol. Chem.* **1983**, *184*, 745.
- (12) Otsu, T.; Matsumoto, A.; Tazaki, T. *Polym. Bull.* **1987**, *17*, 323.
- (13) Otsu, T.; Yoshida, M. *Makromol. Chem. Rapid. Commun.* **1982**, *3*, 127.
- (14) Otsu, T.; Tazaki, T. *Polym. Bull.* **1986**, *16*, 277.
- (15) Cunningham, M. F. *Prog. Polym. Sci.* **2002**, *27*, 1039.
- (16) Qiu, J.; Charleux, B.; Matyjaszewski, K. *Prog. Polym. Sci.* **2001**, *26*, 2083.
- (17) Le, T. P.; Moad, G.; Rizzardo, E.; Thang, S. H. WO 9801478, 1998.
- (18) Prescott, S. W.; Ballard M. J.; Rizzardo, E.; Gilbert, R. G. *Macromolecules* **2002**, *35*, 5417.
- (19) Monteiro, M. J.; de Barbeyrac, J. *Macromolecules* **2001**, *34*, 4416.
- (20) Moad, G.; Chiefari, J.; Chong, Y. K.; Krstina, J.; Mayadunne, R. T. A.; Postma, Almar, Rizzardo, E.; Thang, S. H. *Polym. Int.* **2000**, *49*, 993.
- (21) Monteiro, J. J.; Hodgson, M.; de Brouwer, H. *J. Polym. Sci., Part A: Polym. Chem.* **2000**, *38*, 3864.
- (22) Lansalot, M.; Davis, T. P.; Heuts, J. P. A. *Macromolecules* **2002**, *35*, 7582.
- (23) Hodgson, M. Thesis, University of Stellenbosh, Stellenbosh, South Africa, 2000.
- (24) Wilkinson, T. S.; Boonstra, A.; Montoya-Goni, A.; van Es, S.; Monteiro, M. J.; German, A. L. *J. Colloid Interface Sci.* **2001**, *237*, 21.
- (25) Monteiro, M. J.; Bussels, R.; Wilkinson, T. S. *J. Polym. Sci., Part A: Polym. Chem.* **2001**, *39*, 2813.
- (26) Hong, C. Y.; You, Y. Z.; Bai, R. K.; Pan, C. Y.; Borjihan, G. *J. Polym. Sci., Part A: Polym. Chem.* **2001**, *39*, 3934.
- (27) Quinn, J. F.; Barner, L.; Barner-Kowollik, C.; Rizzardo, E.; Davis, T. P. *Macromolecules* **2002**, *35*, 7620.
- (28) Matyjaszewski, M. *Controlled Radical Polymerization*; ACS Symposium Series 687; American Chemical Society, Washington, DC, 1998; Chapter 1.
- (29) Byun, J.; Cha, J.-Y.; Shim, S. E.; Choe, S. *Polymer (Korea)* **1998**, *22*, 201.
- (30) Stenzel-Rosenbaum, M.; Davis, T. P.; Chen, V.; Fane, A. G. *J. Polym. Sci., Part A: Polym. Chem.* **2001**, *39*, 2777.
- (31) Gaynor, S. G.; Wang, J.-S.; Matyjaszewski, K. *Macromolecules* **1995**, *28*, 8051.
- (32) Young, R. J.; Lovell, P. A. *Introduction to Polymers*, 2nd ed.; Chapman & Hall; London, 1991; Chapter 2.
- (33) Zhang M.; Ray W. H. *Ind. Eng. Chem. Res.* **2001**, *40*, 4336.
- (34) Goodall, A. R.; Winkinson, M. C.; Hearn, J. *J. Polym. Sci., Polym. Chem. Ed.* **1977**, *15*, 2193.
- (35) Myers, D. *Surfactant Science and Technology*; VCH: New York, 1988; Chapter 1.
- (36) Chiefari, J.; Chong, Y. K.; Ercole, F.; Krstina, J.; Jeffery, J.; Le, T. P. T.; Mayadunne, R. T. A.; Meijs, G. F.; Moad, C. L.; Moad, G.; Rizzardo, E.; Thang, S. H. *Macromolecules* **1998**, *31*, 5559.
- (37) Simons, W. W.; Zanger, M. *The Sadtler Guide to the NMR Spectra of Polymers*; Sadtler Research Laboratories: Philadelphia, PA, 1997; p 64.
- (38) Gan, L. M.; Chew, C. H.; Lee, K. C. *Polymer* **1993**, *34*, 3064.
- (39) *Polymer Handbook*, 3rd ed.; Brandrup, J., Immergut, E. H., Eds.; Wiley & Sons: New York, 1989; p V/79.